Research Square

Preprints are preliminary reports that have not undergone peer review.
They should not be considered conclusive, used to inform clinical practice,
or referenced by the media as validated information.

Feasibility study of dose calculation based on contrast-enhanced computed tomography for stereotactic body radiation therapy of lung metastases treated with MR-Linac

Guoqiang Zhao
Sichuan Cancer Hospital &Institute, Sichuan Cancer Center, University of Electronic Science and Technology of China

Min Liu
Sichuan Cancer Hospital &Institute, Sichuan Cancer Center, University of Electronic Science and Technology of China

Yaxin Liu
Sichuan Cancer Hospital &Institute, Sichuan Cancer Center, University of Electronic Science and Technology of China

Junxiang Wu
Sichuan Cancer Hospital &Institute, Sichuan Cancer Center, University of Electronic Science and Technology of China

Hao Guo
Sichuan Cancer Hospital &Institute, Sichuan Cancer Center, University of Electronic Science and Technology of China

Jie Li
Sichuan Cancer Hospital &Institute, Sichuan Cancer Center, University of Electronic Science and Technology of China

Shun Lu
Sichuan Cancer Hospital &Institute, Sichuan Cancer Center, University of Electronic Science and Technology of China

Jinyi Lang
Sichuan Cancer Hospital &Institute, Sichuan Cancer Center, University of Electronic Science and Technology of China

Tiziana Malatesta
Isola Tiberina–Gemelli Isola Hospital

Lintao Li
Sichuan Cancer Hospital &Institute, Sichuan Cancer Center, University of Electronic Science and Technology of China

Xianliang Wang

wangxianliang@scszlyy.org.cn

Sichuan Cancer Hospital &Institute, Sichuan Cancer Center, University of Electronic Science and Technology of China

---

Research Article

Keywords: MR-Linac, contrast-enhanced CT, lung metastases, SBRT, Synthetic CT

Posted Date: June 24th, 2026

DOI: https://doi.org/10.21203/rs.3.rs-9357535/v1

License: This work is licensed under a Creative Commons Attribution 4.0 International License. Read Full License

Additional Declarations: No competing interests reported.

Version of Record: A version of this preprint was published at Radiation Oncology on October 21st, 2026. See the published version at https://doi.org/10.1186/s13014-026-02948-0.

Feasibility study of dose calculation based on contrast-enhanced computed tomography for stereotactic body radiation therapy of lung metastases treated with MR-Linac

Guoqiang Zhao[1, ‡], Min Liu[1, 3, ‡], Yaxin Liu[1], Junxiang Wu[1], Hao Guo[1], Jie Li[1], Shun Lu[1], Jinyi Lang[1], Tiziana Malatesta[2], Lintao Li[1*], Xianliang Wang[1*]

Abstract

Background: The reliability of contrast-enhanced CT (CHCT) as a reference image for MR-based dose calculation in lung stereotactic body radiation therapy (SBRT) with MR-Linac remains uncertain due to contrast-induced electron density (ED) discrepancy. Whether CHCT can be used as a reference image for dose calculation for patients with lung tumors treated with MR-Linac still needs to be explored in further works.

Methods: This retrospective study included 30 patients with lung metastases treated with SBRT (50 Gy in 5 fractions) on a 1.5 T MR-Linac. Non-contrast CT (pCT) and corresponding CHCT acquired in the same respiratory phase were used to extract mean electron density for targets and organs at risk (OARs). The treatment plans (TP_{csCT} and TP_{psCT}) based on synthetic CT (sCT) generated by assigning mean ED derived from pCT and CHCT were recalculated without altering parameters. Dosimetric discrepancy were evaluated using dose-volume histogram metrics, conformity indices, gradient indices and gamma analysis.

Results: Significant differences in mean ED between pCT and CHCT were observed for several structures, most notably the lungs (mean differences >12%), heart, aorta, and bronchial tree ($p < 0.05$), whereas minimal changes were found in bone and spinal cord. Despite these ED variations, dosimetric differences in target coverage were modest, with average discrepancy of 2.21% and 2.31% for TP_{csCT} and TP_{psCT},

respectively. The other dosimetric parameters (D_{max}, $D_{2\%}$, $D_{95\%}$, $D_{98\%}$, D_{mean}, CI and GI) differences for target were generally below 3%. Although statistically significant differences were detected in some OARs dose metrics, all values remained well within clinical tolerance limits (3%).

Conclusion: Despite significant contrast-induced variations in ED, the using of CHCT as a reference image result in minor dosimetric differences in lung SBRT. Considering the patient's financial capacity and the radiation dose from repeated CT scans, CHCT may be used as a reference image for lung tumor SBRT with MR-Linac when clinical risks are appropriately managed.

Keywords: MR-Linac, contrast-enhanced CT, lung metastases, SBRT, Synthetic CT

Min Liu Co-first author

Corresponding author: Xianliang Wang, Lintao Li

E-mail: wangxianliang@scszlyy.org.cn, lilintao@scszlyy.org.cn

Background

The current development of radiation therapy is moving towards high precision, intelligence and individualization, reflecting in image-guided, adaptive therapy-guided personalized treatment strategies[1, 2]. With the rapid advancement of image-guided radiation therapy (IGRT) technology, magnetic resonance-guided radiation therapy (MRgRT) has emerged as a research hotspot in precision radiotherapy due to superior soft tissue resolution, absence of ionizing radiation and ability to monitor target motion in real time[2, 3]. The introduction of MRgRT can significantly improve the accuracy of target localization and the safety of treatment[4].

The precise delivery of radiation therapy plans relies on two core components: accurate target delineation and precise dose calculation. Among these, computed tomography (CT) as an indispensable imaging modality in modern radiation therapy planning offer clear anatomical structure information and reliable tissue electron density (ED) data[5]. Meanwhile, ED exhibits a strong positive correlation with CT values, serving as the foundational core parameter for radiotherapy dose calculation. Treatment planning systems (TPS) estimate tissue ED based on CT values to precisely calculate radiation attenuation patterns and dose distribution[6]. This ensures the prescribed dose is accurately delivered to the target area while maximizing protection of surrounding organs at risk (OARs).

In the clinical design of conventional radiotherapy plans, a well-established clinical convention governs the selection of CT images for target delineation and dose calculation[7]. Contrast-enhanced CT (CHCT) facilitates clear differentiation between tumor and normal tissues through the administration of iodinated contrast agents, particularly for hypervascular tumors and lesions with ill-defined borders[8, 9]. This capability significantly enhances the accuracy and reproducibility of target delineation while reducing the risks of target omission or misdelineation of normal tissues, thereby rendering it widely adopted for target delineation across various tumor types[9]. Nevertheless, non-contrast CT (pCT) eliminates the interference of contrast agents on

ED, as no contrast medium is administered[10, 11]. Additionally, its radiation dose is substantially lower than that of CHCT: the radiation dose of multi-phase CHCT scans exceeds that of non-contrast CT by 30%-50% or even more[12]. Accordingly, non-contrast CT is generally the preferred imaging modality for dose calculation, ensuring the accuracy of dose computation and minimizing the risk of radiation exposure to patients.

However, the conventional imaging selection paradigm faces new challenges and controversies in the clinical application of MRgRT technology[13]. Unlike traditional CT-guided radiotherapy, MRgRT relies on a magnetic resonance linear accelerator (MR-Linac) to achieve the integration of image guidance and treatment[14]. Its dose calculation process still depends on ED provided by CT, as MRI images cannot be directly used for dose calculation due to the lack of ED information[15, 16]. Against this backdrop, there is an urgent need to simplify the imaging workflow in clinical practice, and the using of CHCT for MRgRT dose calculation has emerged as a potential optimization strategy[17]. This approach enables the unification of imaging for both target delineation and dose calculation, eliminating the need for additional non-contrast CT acquisition. It not only reduces patient radiation exposure (avoiding two separate scans: non-contrast and CHCT but also eliminates potential registration errors between CHCT and non-contrast CT[12]. Nevertheless, prior to its clinical implementation, a quantitative assessment of the dosimetric differences between treatment plans based on non-contrast CT and CHCT is required.

This work investigated the potential differences in dosimetry of 30 patients with lung tumors treated with SBRT though MRgART at MR-Linac if CHCT could be used as a reference image for treatment plan, providing valuable insights for clinical practice.

Methods

Patients

This retrospective research included 30 patients with lung cancer who received SBRT treated with MR-Linac at Sichuan Cancer Hospital from August 2021 to June

2025. The basic information of the patients and the treatment details of the target area are summarized in Table 1. This research was approved by the Institutional Ethics Committee (SCCHEC-02-2025-056) of the hospital, and written informed consent was obtained from all patients in this study.

Table 1 Patients and treatment characteristics

Patients	Value
Number	30.0
Years, median (rang)	62.5 (33-85)
Femal-no. (%)	18.0 (60.0%)
Male-no. (%)	12.0 (40.0%)
[a]PTV-no. (%)	
6 cc < Volume < 16 cc	7 (23.3%)
16 cc < Volume < 26 cc	8 (26.7%)
26 cc < Volume < 36 cc	9 (30.0%)
36 cc < Volume < 66 cc	6 (20.0%)
Volume(cc), median (range)	30.6 (6.8-65.3)

[a]PTV: planning target volume; [b]OARs: organ at risk; [c]GTV: gross target volume

Imaging acquisition at simulation CT

The patients were set up in the supine position using positioning aids and immobilized with vacuum pillow (BlueBAG, Elekta AB, Stockholm, Sweden). Next, patients underwent CT scan by Brilliance big bore scanner (Philips Medical System, Cleveland, OH, USA) at the end of exhalation; a first non-contrast CT scan is used for treatment planning, followed a contrast CT scan with the contrast media (CM) to support the physician in delineating the tumor. For CHCT scanning, patients aged under or beyond 63 years received an intravenous injection of iodine iodide of 37 g/100 ml or 32 g/100 ml into the right arm vein, respectively; the injection rate was 2.0 ml/s, and the total injection volume was 1.5 times the patient's body weight (kg). CHCT was acquired 60 s after CM injection during the portal venous phase according to in-house protocol guidelines to obtain optimal visualization of the alveoli and parenchyma of the lung[18, 19]. non-contrast CT and CHCT images were exported to commercial software for automatic OARs contouring (PVmed contourting software, Guangzhou, China) for delineating of all regions of interest (ROIs)[20]; the contoured ROIs and images were

exported to commercial software (MIM Software Inc., Cleveland Ohio, USA), where experienced radiation oncologists delineated the target and verified/modified the automatically segmented OARs.

Reference treatment plan

Target and OARs delineated on MIM commercial software were transferred to Monaco Version 5.4 (Elekta AB, Stockholm, Sweden) for planning. The patients undergo SBRT with Unity 1.5 Tesla MR-linac (Elekta Unity, Elekta AB, Stockholm, Sweden) for a prescribed dose of 50 Gy in 5 fractions. The Monaco Version 5.4 TPS was applied for protocol optimization to achieve the clinical goal of a prescribed dose covering at least 95% of the target volume with a maximum dose in the range of 110-140% of the prescribed dose, and to meet the dose limits of the international guidelines and consensus for OARs as low as possible[21]; the OARs constraints and target volume goals used for plan optimization and validation are shown in Table 2 , with the addition of an indication that the goal would be compromised in case of a conflict between target coverage and OAR constraints. Plans based on pCT scans are optimized using 9~11 beam angles, including ranges from 190° to 350° and 30° to 170°, employing a 2-mm dose grid with a computational uncertainty of 1% per iteration[22]. The reference CT plan contains the ED information of all pixels, and each contour is assigned a corresponding mean ED. These informations are crucial in the online adaptive process, where MRI-based sCT images are used to recalculate the adaptive plan[23].

Table 2 OARs constraints used for lung SBRT delivering 50 Gy in 5 fractions

OAR	Criteria	OAR	Criteria
Spinal cord		**Great Vessels**	
D_{max}	< 30 Gy	D_{max}	< 53 Gy
$D_{0.35cc}$	< 23 Gy	D_{10cc}	< 47 Gy
D_{1cc}	< 14.5 Gy	**Trachea & Prox Bronchi**	
Esophagus		D_{max}	< 32.5 Gy
D_{max}	< 32.5 Gy	$D_{0.5cc}$	< 32 Gy
D_{5cc}	< 19.5 Gy	**Rib**	

Heart		D_{max}	< 43 Gy
D_{max}	< 38 Gy	D_{1cc}	< 35 Gy
$D_{0.5cc}$	< 27 Gy	**Lungs**	
D_{15cc}	< 32 Gy	V_{20Gy}	< 10% Lung-GTV
		D_{1000cc}	< 13.5 Gy (Right and Left)

Abbreviations: OARs, organs at risk; Dmax, maximum point dose; $D_{y\ cc}$, dose received y cubic centimetres; V_{20Gy}, volume covered by a dose of 20 Gy; GTV, gross tumor volume; fx, fraction.

Online adaptive radiotherapy

Each treatment fraction based on MR-Linac starts with the acquisition of the first online MRI, which is used for adaptative plan. The next fraction is adapted and planned based on the reference CT (or MRI scan of the previous treatment fraction), contours, plans, and daily online MRI[2]. The reference CT or MRI is rigidly registered with the online MRI, and the isocenter position in the reference CT is updated; then the adapt to position (ATP) or adapt to shape (ATS) step is performed. Once the OARs or target does not match the patient's daily anatomy, the ATS step is needed. In this case, the main work is to adjust these contours to match anatomy from daily MRI, and the adjusted plan is re-optimized on the daily MR-based sCT. The sCT is used in Monaco TPS to assign average ED using contours drawn on the simulation CT. Daily acquired MRI are deformably registered to the simulation CT, and then all contour information (including average ED and density assignment priority) were applied to the MRI to generate sCT[24]. Unlike the ATS step, the ATP step is mainly aimed at the situation where the OARs or target contours have not been deformed. In the APT step, after the online MRI and the reference CT images are rigidly registered, the plan is directly re-calculated on the reference CT without changing the ROI contour[25]. In both workflows, real-time MRI is required as a plan adjustment in the adaptive workflow.

Use of pCT and CHCT for sCT generation and plan recalculation

The radiation oncologist assessed the concordance of the respiratory phase between the pCT and CHCT scans for each patient to ensure a strong correlation

between the ED and the use of CM. The corresponding ROIs acquired by delineating pCT and CHCT images with MIM software were imported into Monaco TPS to evaluate and obtain the average ED of each structure (including the target). For each patient, each ROI depicted on pCT was assigned average ED obtained on pCT and CHCT to form psCT and csCT, as shown in Fig.1. Without changing any planning parameters, the reference treatment plan was recalculated with psCT and csCT images to obtain the sCT treatment plan (TP_{psCT} and TP_{csCT}).

sCT and pCT plan comparison

Target and OARs dose volume histogram (DVH) were used as the main indicators to evaluate the TP_{pCT}, TP_{psCT} and TP_{csCT}. The target volume received by 100% of the prescribed dose (V_{Dpre}), the dose received by 2%, 95% and 98% of the volume ($D_{2\%}$, $D_{95\%}$ and $D_{98\%}$), as well as the maximum, minimum and mean doses (D_{max}, D_{min} and D_{mean}) were collected. In addition, the conformity index (CI) and gradient index (GI) were evaluated. The CI is defined as the square of PTV inside the prescribed dose divided by volume of the prescribed dose multiplied the planning target volume[26]. The GI is defined as the ratio of the volume receiving 50% of the prescription dose ($V_{50\%}$) to the PTV[13]. For OARs, the dose in x cm^3 or x% volume (D_{xcc}, $D_{x\%}$) and D_{max} are used. V_{Dpre} is described in percentage point, and the difference is obtained by subtracting the value of TP_{sCT} from the dosimetric parameter corresponding to TP_{pCT}; the dosimetric parameter expressed in Gy considers the percentage of the dose difference between the two.

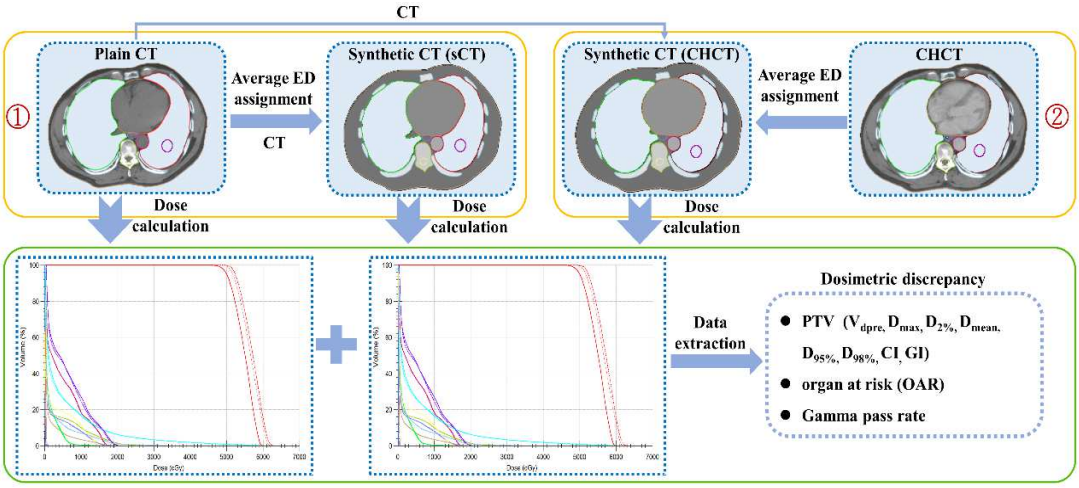


Fig.1 Flowchart and schematic diagram of this work

Gamma analysis was used to evaluate target and OARs dose distribution information, with a standard of 2%-2 mm and a lower dose threshold of 5% of the prescription dose by CERR v4.4 (https://github.com/cerr/CERR). We sought to keep the overall dosimetric differences between treatment plan and plan based on sCT dose as low as possible, and the sCT treatment plan recalculated based on the reference CT were considered concordant when the plan had an $\gamma < 1$ above the 99% with criterion and the dose difference at any point in the DVH was less than 1.5% or 1 Gy[14].

SPSS version 25.0 (IBM, Armont, USA) was used to analyze patient and plan data. The dosimetric parameters of TP_{psCT}, TP_{csCT} and TP_{pCT} were analyzed using t-test or Wilcoxon rank-sum depending on the results of the normality test; $p < 0.05$ was considered statistically significant.

Results

The mean ED of ROIs (spinal cord, heart, ribs, lung_L, lung_R, lung-GTV, esophagus, aorta, bone, bronchial tree and liver) based on non-contrast CT and corresponding CHCT were calculated from 30 patients and were shown in Table 3 along with their comparison. The reference ED for various tissues were reported with the international standards from radiation therapy and radiological protection ICRU Report 46 and ICRP 110; these ED are relative values determined by the absolute ratio of the tissue to that of water[27].

Table 3 Electron density and comparison for ROIs obtained from non-contrast CT and CHCT

ROIs	Ref.	pCT	CHCT	Max Diff (%) (pCT *VS* CHCT)	Mean Diff (%) (pCT *VS* CHCT)	*p*
Spinalcord	1.04	1.04±0.01	1.04±0.00	0.70	0.33±0.28	< 0.001
Heart	1.04	1.03±0.01	1.08±0.01	6.17	3.45±1.03	< 0.001
Rib	1.44	1.19±0.00	1.19±0.00	0.26	0.21±0.19	< 0.001
Lung_L	0.26	0.29±0.05	0.32±0.06	18.75	12.03±5.89	< 0.001
Lung_R	0.26	0.28±0.04	0.31±0.05	20.38	13.36±4.98	< 0.001
Lung-GTV	0.26	0.28±0.05	0.32±0.04	19.86	12.86±5.03	< 0.001
Esophagus	1.04	0.95±0.01	0.96±0.00	3.16	1.95±0.63	< 0.001
Aorta	1.04	1.05±0.03	1.12±0.04	9.18	5.21±3.65	< 0.001
Bone	1.15	1.17±0.01	1.17±0.01	0.44	0.30±0.28	< 0.001
BronchialTree	0.50	0.51±0.01	0.52±0.01	8.42	4.69±3.85	< 0.001
liver	1.05	1.07±0.01	1.08±0.01	1.72	1.09±0.65	< 0.001

In Fig.2, pCT, CHCT and corresponding generated sCT transversal images of a representative patient are shown. The ED of structures in CHCT and corresponding sCT images are higher than these in pCT, with specific values shown in Table 3. A discrepancy exists in the ED value obtained from pCT for the rib region from the different way of delineation used compared with that suggested by ICRU 46[27]. The mean ED of each structure obtained from CT and CHCT showed significant differences ($p < 0.05$) with larger difference for lungs (18.75%, 20.38% and 19.86 for the left lung, right lung and lung-GTV), aorta (9.18%), heart (6.17%) and bronchial tree (8.42%) than other structure as shown in Fig.3. Meanwhile, the differences of mean ED for each ROIs from CT and CHCT exhibited varying average magnitudes, with the larger deviations registered (> 10%) for the lung (12.03%, 13.36% and 12.86% for the left lung, right lung and lung-GTV).

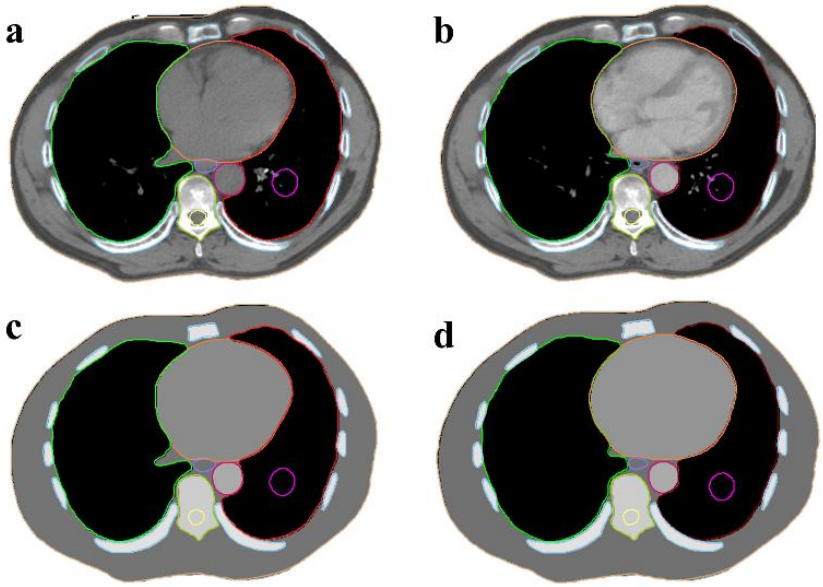


Fig.2 (a-b) Non-contrast CT and CHCT as well as (c-d) corresponding synthetic CT images for a same patient

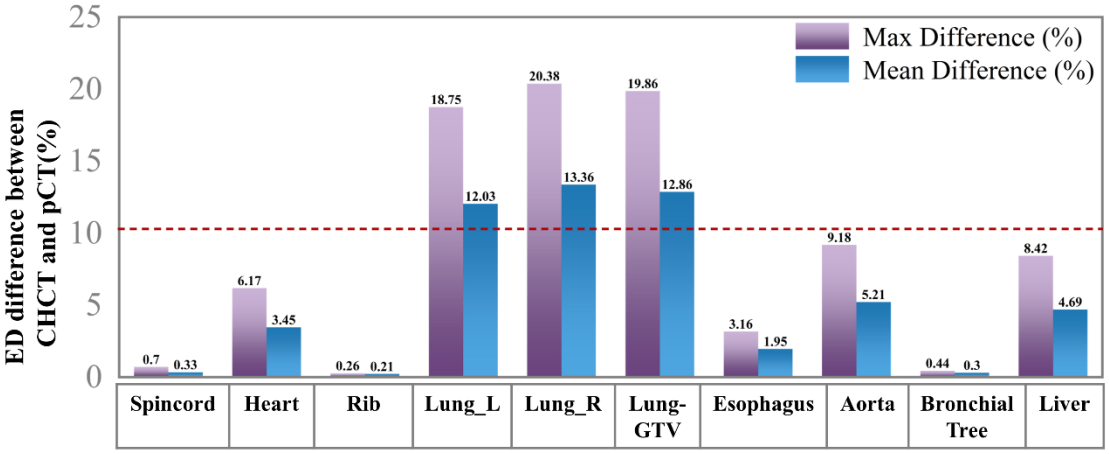


Fig.3 The max and mean difference of electrons density for ROIs obtained from non-contrast CT and CHCT

The DVH parameters of the target and OARs in 90 delivered plans (TP_{csCT}, TP_{pCT} and TP_{psCT} for each patients) for 30 patients were compiled and presented in Table S1 (Supporting Information). Among the 30 TP_{pCT} plans, 26 met clinical requirements for both target coverage and OARs constraints except 4 patients exhibited lower target coverage ($84\% < V_{Dpre} < 90\%$) due to the positioning of target close to the ribs in order to satisfy OARs constraints. The dose distribution and differences of target and OARs among TP_{csCT}, TP_{pCT} and TP_{psCT} were shown in Fig.4-5. The DVH and dose distributions in pCT and sCT based on mean ED obtained from pCT and CHCT are

shown in Fig.4. The DVH curves for the target in the TP_{psCT} and TP_{csCT} plan exhibit significant dosimetric differences compared to those in the TP_{pCT} plan. However, these parameters did not show significant discrepancies between the two plans based on synthetic CT. Moreover, for each patient studied, the liver received doses below 2.5 Gy ($5\%D_{pre}$) in three treatment plans compared and have not been included.

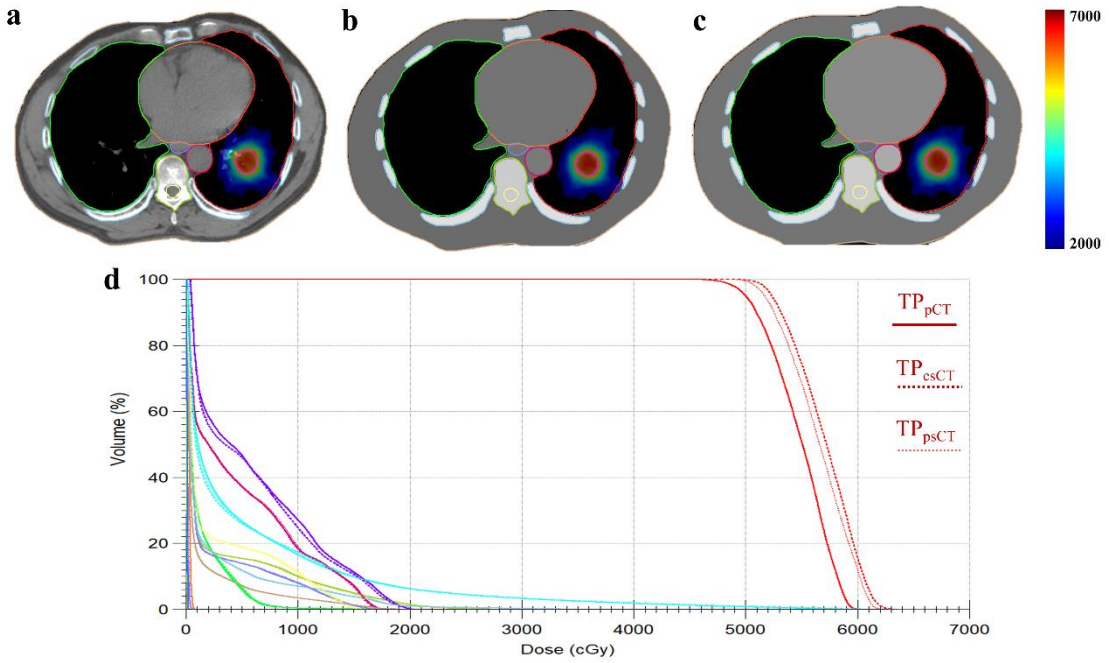


Fig.4 Dose distribution of (a) TP_{pCT}, (b) TP_{psCT} and (c) TP_{csCT} in transversal image and (d) DVH comparison for a representative patient

The differences in the dose-volume metrics of PTV and OARs among TP_{csCT}, TP_{pCT} and TP_{psCT} were shown in Fig.5. Among the parameters, the dosimetric parameters of the target exhibit larger variations compared to those of the OARs. The greatest dosimetric discrepancies were observed in $D_{98\%}$ of PTV, with 3.06% (TP_{csCT} *VS* TP_{pCT}) and 2.89% (TP_{psCT} *VS* TP_{pCT}), respectively. Moreover, the corresponding of TP_{csCT} and TP_{psCT} results showed differences in target coverage with average values of 2.21% (TP_{csCT} *VS* TP_{pCT}) and 2.31% (TP_{psCT} *VS* TP_{pCT}). Except the GI of the target, each parameter (V_{Dpre}, D_{max}, $D_{2\%}$, $D_{95\%}$, $D_{98\%}$, D_{mean}, CI) derived from TP (TP_{csCT}, TP_{pCT} and TP_{psCT}) showed significant differences ($p < 0.05$).

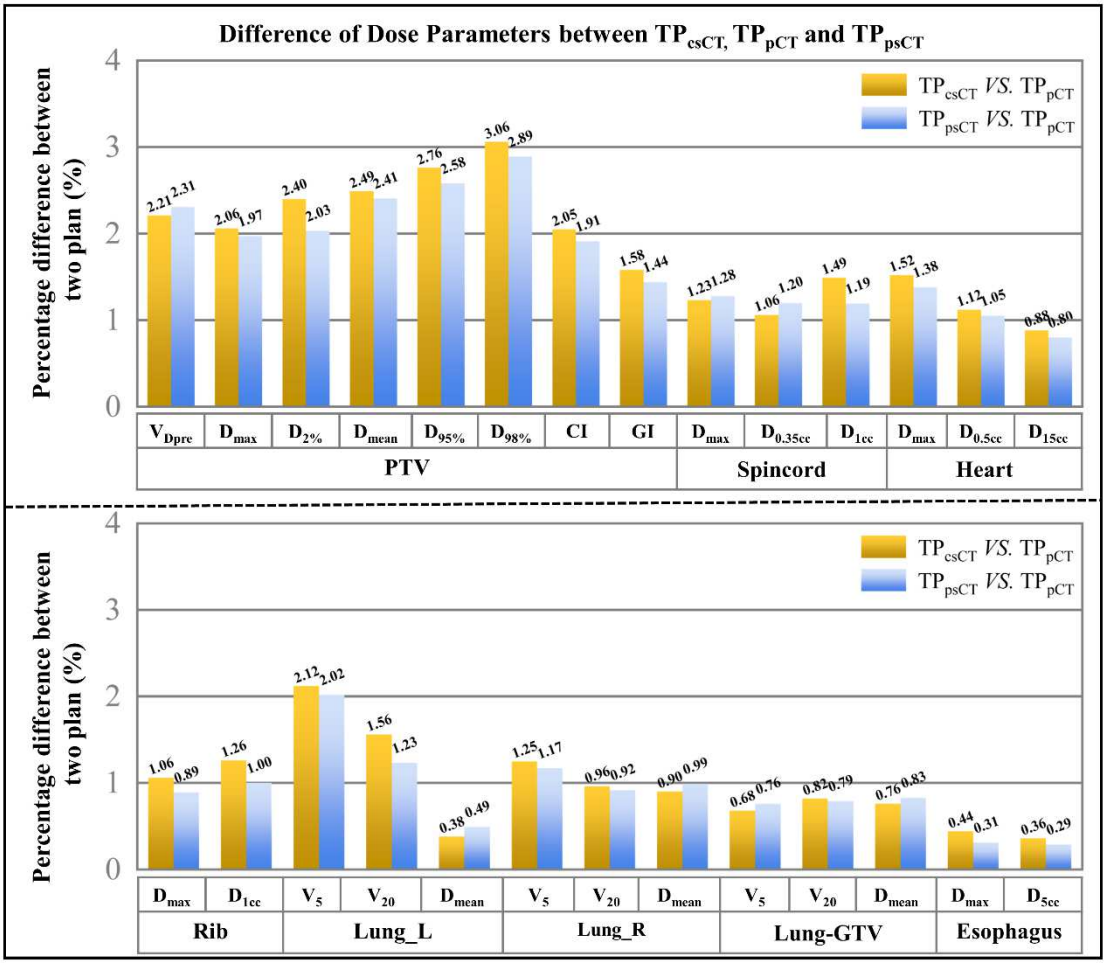


Fig.5 Differences in the investigated dose-volume metrics of PTV and OARs among TP_{csCT}, TP_{pCT} and TP_{psCT}.

For OARs, their position respect to the target was far enough away not to affect dosimetry, except for the 4 patients where the target near by the ribs, and the size of target respect to the OARs was small, resulting the radiation doses received for these OARs fell below the limits indicated in international guidelines. As a result, even though significant differences ($p < 0.05$) were found between TP_{csCT} and TP_{pCT} as well as TP_{psCT} and TP_{pCT} for the spinal cord D_{max}, heart D_{max} and $D_{0.5cc}$, lung (left lung, right lung and lung-GTV) V_5, V_{20} and D_{mean}, the dose received remains so below the OARs limits that these discrepancies are not clinically appreciable.

Fig.6 displays the results of global gamma analysis for the dose distribution of the TP_{csCT}, TP_{psCT} and TP_{pCT} plan with the PTV, spinal cord, heart, rib, lung_L, lung_R, lung-GTV and esophagus, confirm the discrepancies found using the comparison of the

DVH dosimetric parameters and the statistical analysis. In the 3 mm/3% criteria, the average gamma passing rate for the PTV and OARs exceeded 95%, with only the PTV pass rate being slightly lower than that of other OARs.

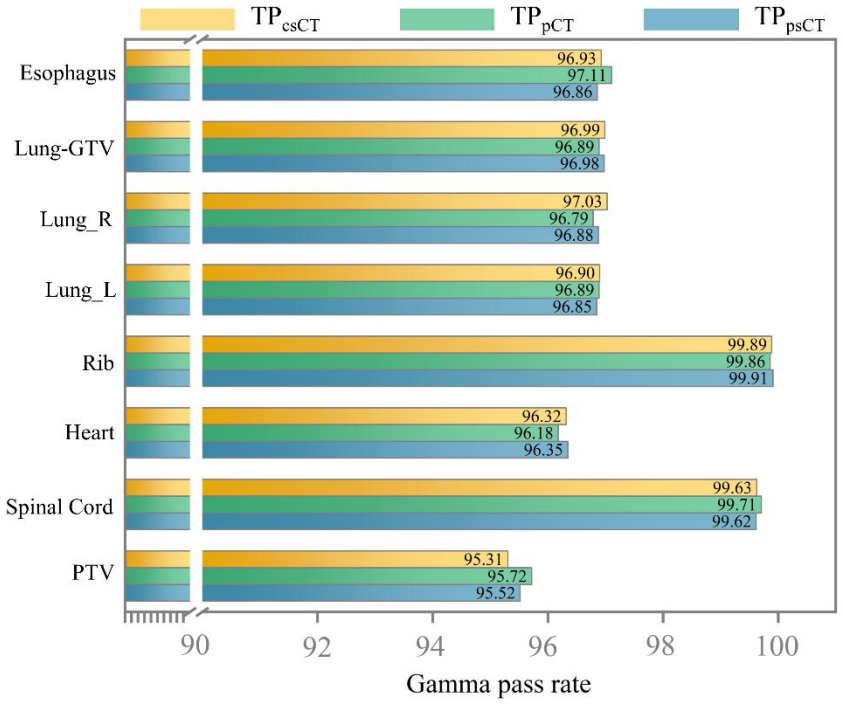


Fig.6 Average gamma passing rates of the TP_{csCT}, TP_{pCT} and TP_{psCT} plans measured with 3%-3mm criteria

Discussion

CM are widely used in radiation therapy for the delineation of target and OARs based on CHCT to improve the delineation accuracy[8, 13, 28]. However, using CHCT images for delivered plans may result in dosimetric discrepancies due to differences in ED compared to non-contrast CT scans[28]. The daily adaptive plans are treated based on MR-based sCT or reference CT for the ATS or ATP workflow at unity MR-linac[2]. In both cases, the mean ED values obtained from the reference CT are applied in the daily plan calculation. Therefore, whether CHCT can be used as a reliable reference CT image compared with non-contrast CT for adaptive planning at unity MR-linac is crucial.

According to the results of this work, it is different significantly for the mean ED of OARs such as heart, lungs, aorta and bronchial tree between obtained from CHCT

and pCT. This arises in mean ED results from the intravenous injection of CM, which are transported throughout via the bloodstream and highly concentrated within these tissues[29]. The average ED of the esophagus is raised due to contouring bias caused by changes in HU values of surrounding aorta and heart[30]. The liver accumulates contrast agents due to it filters blood, but the spinal cord, ribs, and other structures are less affected[31].

However, when comparing the dosimetric parameters of lung SBRT plans across TP_{csCT}, TP_{pCT} and TP_{psCT}, significant impact in target dosimetry was fund for only 2 patients out of 30 patients. The notable difference in the target dosimetry parameters were 5.73% for D_{max} and 6.61% for $D_{2\%}$, with the average discrepancie values less than 3%, also for left Lung V_5, other OARs dosimetric parameter were less than 2%. The impact of using CHCT as the reference CT on plan dosimetry remains minimal in a cohort of 30 patients, even with a greater effect on the average ED for OARs. Notably, in TP_{pCT}, the CI of target is lower and the D_{max} of target is higher compared to these in TP_{csCT} and TP_{psCT} due to the electron return effect (ERE) at the tissue-air interface of the lung[32-34]. The density differences at tissue-air interfaces are preserved in the TP_{pCT} plan. This increases the dose deposition in adjacent tissues due to the magnetic field causes secondary electrons to spiral and return to the interface. Therefore, dose homogeneity decreased in the TP_{pCT}, with occurrence of hot spots within the PTV.

The delivered plan was designed with X-ray radiation primarily through the lungs, and even the contrast agent induced average ED variation exceeding 10% in the lungs (12.03% for left lung, 13.36% for right lung and 12.86% for lung-GTV), resulting the discrepancy in target dose coverage remained less than 3%. This is more than that reported in previous literature for pelvi treatment planning, where a single population-based relative electron density assignment resulted in down to ±0.8% differences[3]. This discrepancy originates from the fact that the average ED of the lungs and heart are more significantly affected by contrast agents than that of the pelvis and surrounding OARs[35].

Nevertheless, the well-known risks associated with CM must be considered, including potential allergic reactions and increased costs. In lung metastasis patients, beyond patients with pre-existing kidney disease, special caution should also be exercised in elderly individuals, patients with diabetes or cardiovascular disease, those receiving nephrotoxic systemic therapies, malnourished or dehydrated cancer patients, and individuals with thyroid dysfunction or prior contrast reactions[36]. In image-guided radiotherapy, repeated contrast exposure may further amplify these risks, even in patients with preserved baseline renal function.

Gamma pass rate is calculated to validate the dose variation induced by the assignment of average electron density with CM discussed earlier in the TP_{csCT}, TP_{pCT} and TP_{psCT} plan. Our analysis revealed that the gamma passing rate for the three plans exceeded 95% under the 3%-3mm tolerance limits. The gamma pass rates of ribs and spinal cord exceeding 99% in all plans compared to other OARs and target due to their electron density is not entirely dependent on contrast agents. This level of performance is widely considered acceptable in clinical practice[37].

Several limitations were fund in this study. First, the statistical power and generalizability of the findings are constrained due to the relatively small patient cohort. The time interval between contrast agent injection and CT scanning affects organ visibility and contour delineation. The single-institution study setting further limits the diversity of patient demographics and tumor characteristics. Nevertheless, variations in the interval between CT scanning and contrast agent administration may introduce bias in effective ED, thereby compromising the accuracy of dose assessments. Additionally, although we opted to acquire CT and CHCT scans during the same breath phases, this may still result in slight respiratory phases differences and introduce additional uncertainty in average ED extraction[38].

Our work underscores several important aspects. First, the use of CHCT leads to minor dosimetric discrepancy in SBRT plans for lung metastasis. Second, the dosimetric consistency of OARs was demonstrated to remain consistent, with small

dosimetric discrepancy coexisting alongside significant difference, demonstrating that CHCT and CT provide reliable information for OARs without compromising the accuracy of the delivered plan. Crucially, while significant deviations found in the average ED of the lungs, which does not significantly impact the overall dose distribution for the delivered plan. Using the CHCT as the reference scan does not significantly impact the overall dose distribution of the plan. Future research should consider larger, multi-institutional cohort studies employing standardized imaging protocols to mitigate these limitations and provide more comprehensive insights into the role of CHCT in radiation therapy.

Conclusion

The use of CHCT as a reference image in lung SBRT treatment plan results in minor dose deviations for both the target and OARs compared to non-contrast CT. Considering the patient's financial capacity and the radiation dose from repeated CT scans, CHCT could be served as an alternative reference image in certain clinical scenarios. However, its application should be investigated within a broader clinical framework and tailored to individualized treatment strategies.

Abbreviations

CT	Computed tomography
CHCT	Contrast-enhanced computed tomography
SBRT	Stereotactic body radiation therapy
MR-Linac	Magnetic resonance linear accelerators
ED	Electron density
ROIs	Regions of interest
pCT	non-contrast CT
sCT	Synthetic computed tomography
DVH	Dose volume histogram

1	TP_{pCT}	The original treatment plan
2	TP_{csCT}	The sCT treatment plan that electron density obtained from CHCT
3	TP_{psCT}	The sCT treatment plan that electron density obtained from pCT
4	VDpre	Target volume covered by the prescribed dose
5	CI	The conformity index
6	GI	The gradient index
7	OAR	Organs at risk
8	CM	Contrast media
9	MR	Magnetic resonance
10	ATS	Adapt to shape
11	ATP	Adapt to position
12	MRI	Magnetic resonance imaging
13	MRgART	Magnetic resonance-guided adaptive radiotherapy
14	TPS	Treatment planning system
15	ICRU	The International Commission on Radiation Units and Measurements
16	ICRP	The International Commission on Radiological Protection
17	PTV	Planning target volume
18	GTV	Gross target volume

19 ## Acknowledgements

20 None.

21 ## Author contributions

22 Study concept and design of the Research: GQZ, ML, XLW, SL, JYL, TM; Acquisition
23 of data and images dataset processing: GQZ, ML, YXL, HG; Analysis and
24 interpretation of data: GQZ, JL, LTL, JXW, HG; Manuscript Preparation: ML, GQZ;
25 Writing Manuscript GQZ, XLW; Manuscript critical revision: GQZ, ML, YXL, JXW,
26 JL, LTL, XLW, TM; All authors read and approved the final manuscript.

Funding

Sichuan Cancer Hospital Outstanding Youth Fund, China, YB2025014.

Young Scientists Fund of the Natural Science Foundation of China, No.12505391

Data availability

No datasets were generated or analysed during the current study.

Declarations

Ethics approval and consent to participate

The authors declare that this retrospective study “Feasibility study of dose calculation based on contrast-enhanced CT for SBRT of lung metastases treated with MR-Linac” received the approval of the ethic committee of Sichuan Cancer Hospital located in 55th Renmin South Road, 4th Section, 610041, Chengdu, China (Approval number SCCHEC-02-2025-056). This study was conducted in accordance with the Declaration of Helsinki.

Consent for publication

Even if no individual patient data were reported, consensus has been received by every patient for the elaboration of its data and for future scientific publication.

Competing interests

The authors declare no competing interests.

Author details

[1]Department of Radiation Oncology, Radiation Oncology Key Laboratory of Sichuan Province, Sichuan Clinical Research Center for Cancer, Sichuan Cancer Hospital &Institute, Sichuan Cancer Center, University of Electronic Science and Technology of China, Chengdu, China

[2]Medical Physics Unit, Department of Radiotherapy and Medical Oncology and Radiology, Isola Tiberina–Gemelli Isola Hospital, Rome, Italy

[3]College of Computer Science and Cyber Security, Chengdu University of Technology,

1 Chengdu, China

2

References

1. Baskar R, Lee KA, Yeo R, Yeoh K. Cancer and radiation therapy: current advances and future directions. Int J Med Sci. 2012;9(3):193-9.
2. Ocanto A, Torres L, Montijano M, Rincón D, Fernández C, Sevilla B, et al. MR-LINAC, a new partner in radiation oncology: current landscape. Cancers (Basel). 2024;16(2):270.
3. Carr ME, Jelen U, Picton M, Batumalai V, Crawford D, Peng V, et al. Towards simulation-free MR-linac treatment: utilizing male pelvis PSMA-PET/CT and population-based electron density assignments. Phys Med Biol. 2023;68(19):195012.
4. Dona Lemus OM, Cao M, Cai B, Cummings M, Zheng D. Adaptive radiotherapy: next-generation radiotherapy. Cancers (Basel). 2024;16(6):1206.
5. Constantinou C, Harrington JC, DeWerd LA. An electron density calibration phantom for CT-based treatment planning computers. Med Phys. 1992;19(2):325-7.
6. Seco J, Evans PM. Assessing the effect of electron density in photon dose calculations. Med Phys. 2006;33(2):540-52.
7. Mackie TR, Kapatoes J, Ruchala K, Lu W, Wu C, Olivera G, et al. Image guidance for precise conformal radiotherapy. Int J Radiat Oncol Biol Phys. 2003;56(1):89-105.
8. Yang X, Liu M, Ren Y, Chen H, Yu P, Wang S, et al. Using contrast-enhanced CT and non-contrast-enhanced CT to predict EGFR mutation status in NSCLC patients—a radiomics nomogram analysis. Eur Radiol. 2022;32(4):2693-703.
9. Haghparast M, Jamil F, Darvish L. The effect of contrast agent on dose distribution in treatment planning radiotherapy: a systematic review. J Med Imaging Radiat Sci. 2025;56(5):101910.
10. Al-Buriahi MS, Tonguc BT. Mass attenuation coefficients, effective atomic numbers and electron densities of some contrast agents for computed tomography. Radiat Phys Chem Oxf Engl 1993. 2020;166:108507.
11. Lusic H, Grinstaff MW. X-ray-computed tomography contrast agents. Chem Rev. 2013;113(3):1641-66.
12. Kalra MK, Maher MM, Toth TL, Hamberg LM, Blake MA, Shepard J, et al. Strategies for CT radiation dose optimization. Radiology. 2004;230(3):619-28.
13. Liu M, Liu M, Yang F, Liu Y, Wang S, Chen Y, et al. Impact of contrast-enhanced CT in the dosimetry of SBRT for liver metastases treated with MR-linac. Radiat Oncol. 2024;19(1):144.
14. Fong SC, Lau E, Liu DS, Tebbutt NC, Khor R, Leong T, et al. MR-guided radiotherapy in oesophageal cancer: from principles to practice—a narrative review. Curr Oncol. 2026;33(1):34.
15. Seco J, Evans PM. Assessing the effect of electron density in photon dose calculations. Med Phys. 2006;33(2):540-52.
16. Hoffmann A, Oborn B, Moteabbed M, Yan S, Bortfeld T, Knopf A, et al. MR-guided proton therapy: a review and a preview. Radiat Oncol. 2020;15(1):129.
17. Karotki A, Mah K, Meijer G, Meltsner M. Comparison of bulk electron density and voxel-based electron density treatment planning. J Appl Clin Med Phys. 2011;12(4):3522.
18. McCollough CH, Rajendran K, Baffour FI, Diehn FE, Ferrero A, Glazebrook KN, et al. Clinical applications of photon counting detector CT. Eur Radiol. 2023;33(8):5309-20.
19. Wu G, Woodruff HC, Shen J, Refaee T, Sanduleanu S, Ibrahim A, et al. Diagnosis of invasive lung adenocarcinoma based on chest CT radiomic features of part-solid pulmonary nodules: a

multicenter study. Radiology. 2020;297(2):451-8.
20. Yu X, He L, Wang Y, Dong Y, Song Y, Yuan Z, et al. A deep learning approach for automatic tumor delineation in stereotactic radiotherapy for non-small cell lung cancer using diagnostic PET-CT and planning CT. Front Oncol. 2023;13:1235461.
21. Benedict SH, Yenice KM, Followill D, Galvin JM, Hinson W, Kavanagh B, et al. Stereotactic body radiation therapy: the report of AAPM task group 101. Med Phys. 2010;37(8):4078-101.
22. Snyder JE, St-Aubin J, Yaddanapudi S, Boczkowski A, Dunkerley DAP, Graves SA, et al. Commissioning of a 1.5t elekta unity MR-linac: a single institution experience. J Appl Clin Med Phys. 2020;21(7):160-72.
23. Bahloul MA, Jabeen S, Benoumhani S, Alsaleh HA, Belkhatir Z, Al-Wabil A. Advancements in synthetic CT generation from MRI: a review of techniques, and trends in radiation therapy planning. J Appl Clin Med Phys. 2024;25(11):e14499.
24. Boulanger M, Nunes J, Chourak H, Largent A, Tahri S, Acosta O, et al. Deep learning methods to generate synthetic CT from MRI in radiotherapy: a literature review. Phys Med. 2021;89:265-81.
25. Feng X, Tang B, Yao X, Liu M, Liao X, Yuan K, et al. Effectiveness of bladder filling control during online MR-guided adaptive radiotherapy for rectal cancer. Radiation oncology (London, England). 2023;18(1):136.
26. Wilke L, Moustakis C, Blanck O, Albers D, Albrecht C, Avcu Y, et al. Improving interinstitutional and intertechnology consistency of pulmonary SBRT by dose prescription to the mean internal target volume dose. Strahlentherapie und Onkologie : Organ der Deutschen Rontgengesellschaft ... [et al]. 2021;197(9):836-46.
27. Scott JA. Photon, electron, proton and neutron interaction data for body tissues. Journal of Nuclear Medicine January. 1993;34(1):171.
28. Mazloumi M, Van Gompel G, Kersemans V, de Mey J, Buls N. The presence of contrast agent increases organ radiation dose in contrast-enhanced CT. Eur Radiol. 2021;31(10):7540-9.
29. Jiang Z, Zhang M, Li P, Wang Y, Fu Q. Nanomaterial-based CT contrast agents and their applications in image-guided therapy. Theranostics. 2023;13(2):483-509.
30. Linde P, Mallmann M, Adams A, Wegen S, Rosenbrock J, Trommer M, et al. Chemoradiation for elderly patients (≥65 years) with esophageal cancer: a retrospective single-center analysis. Radiat Oncol. 2022;17(1):187.
31. Liu B, Xu Y, Zhang X, Qi W, Ren B, Kong W, et al. A contrast-enhanced CT histogram-driven nomogram for predicting post-radiotherapy liver regeneration in hepatocellular carcinoma. Radiat Oncol. 2025;20(1):159.
32. Shortall J, Vasquez Osorio E, Chuter R, Green A, McWilliam A, Kirkby K, et al. Characterizing local dose perturbations due to gas cavities in magnetic resonance-guided radiotherapy. Med Phys. 2020;47(6):2484-94.
33. Shortall J, Vasquez Osorio E, Aitkenhead A, Berresford J, Agnew J, Budgell G, et al. Experimental verification the electron return effect around spherical air cavities for the MR-linac using monte carlo calculation. Med Phys. 2020;47(6):2506-15.
34. Huang CY, Yang B, Lam WW, Geng H, Cheung KY, Yu SK. Magnetic field induced dose effects in radiation therapy using MR-linacs. Med Phys. 2023;50(6):3623-36.
35. Olinger K, Liu X, Khoshpouri P, Khoshpouri P, Scoutt LM, Khurana A, et al. Added value of contrast-enhanced US for evaluation of female pelvic disease. Radiographics. 2024;44(2):e230092.
36. Mahajan A, Gupta A, Shukla S, Agarwal U, Rai P, Sable N, et al. Additional use of extrinsic

warmer for intravenous CT contrast media and its impact on incidence of contrast extravasations and allergic like reactions: a prospective observational case control study. Clin Radiol. 2024;79(11):851-60.

37. Rostami A, Neto AJDC, Paloor SP, Khalid AS, Hammoud R. Comparison of four commercial dose calculation algorithms in different evaluation tests. J Xray Sci Technol. 2023;31(5):1013-33.
38. Kalisz K, Navin PJ, Itani M, Agarwal AK, Venkatesh SK, Rajiah PS. Multimodality imaging in metabolic syndrome: state-of-the-art review. Radiographics. 2024;44(3):e230083.

Supplementary Files

This is a list of supplementary files associated with this preprint. Click to download.

- SupportingInformation.docx